Bioorganic & Medicinal Chemistry 27 (2019) 3167–3178

Contents lists available at ScienceDirect

Bioorganic & Medicinal Chemistry

journal homepage: www.elsevier.com/locate/bmc

Defined concatenated α6α1β3γ2 $GABA_A$ receptor constructs reveal dual action of pyrazoloquinolinone allosteric modulators

X. Simeone[a,1], M.T. Iorio[b,1], D.C.B. Siebert[b], S. Rehman[a], M. Schnürch[b], M.D. Mihovilovic[b], M. Ernst[a,*]

[a] Department of Molecular Neurosciences, Center for Brain Research, Medical University of Vienna, Spitalgasse 4, 1090 Wien, Austria
[b] Institute of Applied Synthetic Chemistry, TU Wien, Vienna, Austria

ARTICLE INFO

Keywords:
$GABA_A$ receptor
Pyrazoloquinolinones
Allosteric modulation
Concatenation

ABSTRACT

Pyrazoloquinolinones (PQs) have been extensively studied as modulators of $GABA_A$ receptors with different subunit composition, exerting modulatory effects by binding at α+/β- interfaces of $GABA_A$ receptors. PQs with a substituent in position R7 have been reported to preferentially modulate α6- subunit containing $GABA_A$ receptors which are mostly expressed in the cerebellum but were also found in the olfactory bulb, in the cochlear nucleus, in the hippocampus and in the trigeminal sensory pathway. They are considered potentially interesting in the context of sensori-motor gating deficits, depressive-like behavior, migraine and orofacial pain. Here we explored the option to modify the lead ligands' R7 position. In the compound series we observed two different patterns of allosteric modulation in recombinantly expressed α6β3γ2 receptors, namely monophasic and biphasic positive modulation. In the latter case the additional phase occurred in the nanomolar range, while all compounds displayed robust modulation in the micromolar range. Nanomolar, near silent binding has been reported to occur at benzodiazepine binding sites, but was not investigated at the diazepam insensitive α6+/γ2- interface. To clarify the mechanism underlying the biphasic effect we tested one of the compounds in concatenated receptors. In these constructs the subunits are covalently linked, allowing to form either the α6+/γ2- interface, or the α6+/β3- interface, to study the resulting modulation. With this approach we were able to ascribe the nanomolar modulation to the α6+/γ2- interface. While not all compounds display the nanomolar phase, the strong modulation at the α6+/β3 interface proved to be tolerant for all tested R7 groups. This provides the future option to introduce e.g. isotope labelled or fluorescent moieties or substituents that enhance solubility and bioavailability.

1. Introduction

$GABA_A$ receptors ($GABA_A$Rs) are a class of receptors belonging to a superfamily of pentameric ligand-gated ion channels. The five subunits are identical in case of homopentameric receptors, or belong to different subunit classes in case of heteropentamers. So far, nineteen genes coding for different subunits that are grouped into eight classes (α1–6, β1–3, γ1–3, δ, ε, θ, π and ρ1–3) have been identified in mammalians. Even though heteropentameric assembly leads to huge subtype heterogeneity, it is believed that the most common receptors are composed of two α and two β subunits together with one γ subunit.[1] These receptors are targets of many clinically used compounds such as intravenous and volatile anesthetics or benzodiazepines (BZs).[2–5] The latter modulate agonist function via an allosteric binding site at the interface between the α+ and the γ- subunit faces of the extracellular domain.

Among the allosteric modulators identified so far, pyrazoloquinolinones (PQs) have been extensively studied in the last decades for their interesting pharmacological profile.[6–8] It has been reported that compounds belonging to the class of PQs bind at two different extracellular interfaces of the $GABA_A$R with different affinities: at lower concentrations, the binding at the interface α+/γ- (high affinity BZ- site, here PQnM) results in no or very weak modulation of the receptor, while the increase of the concentration leads to a positive current modulation due to the interaction at the α+/β- interface (low affinity PQ–site) Fig. 1[6].

In previous studies some PQ derivatives with substituents in the R7 position have been identified as functionally selective for α6β3γ2 over

* Corresponding author.
E-mail address: margot.ernst@meduniwien.ac.at (M. Ernst).
[1] These authors contributed equally.

https://doi.org/10.1016/j.bmc.2019.06.006
Received 21 December 2018; Received in revised form 8 May 2019; Accepted 3 June 2019
Available online 05 June 2019
0968-0896/

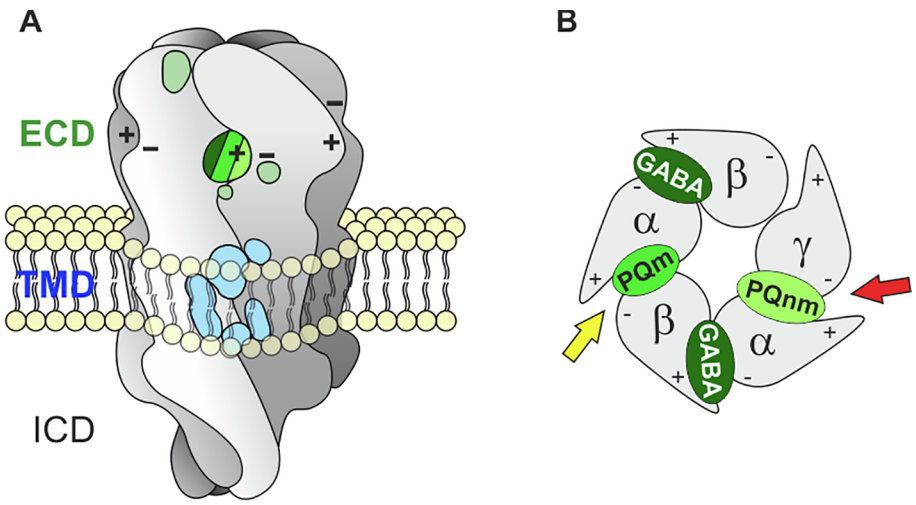

Figure 1. Schematic side and top view of a generic $GABA_A$ receptor pentamer with its extracellular (ECD), transmembrane (TMD) and intracellular (ICD) domains and their binding sites. **A)** Side view of a generalized $GABA_A$ receptor embedded in the cell membrane. The interfaces are formed by a principal (plus) subunit and a complementary (minus) subunit. ECD sites are displayed in shades of green, TMD sites in shades of blue [1]. Several ligands use both the ECD and TMD sites, like diazepam [5] and some PQs [8]. Sites not involved in this study are light green (ECD) and light blue (TMD). **B)** Top view of the ECD, the subunit arrangement is the one generally accepted for the most common subtype containing α1, β2 and γ2 subunits. In the ECD, GABA binds at the β+/α- interface present twice, benzodiazepines bind at α+/γ- and pyrazoloquinolinones bind at α+/β-, where they exert positive allosteric modulation of the receptor through low affinity binding (yellow arrow, PQm–site). PQs additionally bind with high affinity at α+/γ- (red arrow, PQnm–site), where they are mainly silent (null modulatory) binders.

α1–5β3γ2 receptors. So far, the introduction of a methoxy– or a bromo-group has led to this particular α6 selectivity profile.[9,10].

$GABA_A$Rs containing α6 subunits are mostly expressed in the cerebellum[11,12], where they have been detected in granule cells in synaptic and extra–synaptic localizations.[13]. They also occur in the olfactory bulb and the cochlear nucleus.[14] Recently, α6–containing receptors have also been detected in the hippocampus and associated with depressive–like symptoms.[15] The interest towards these receptors increased further as they have been reported to contribute in alleviation of sensori- motor gating deficits[9] and to exist in trigeminal ganglia[16] where they seem to be involved in orofacial pain and migraine.[17]

In cerebellar granule cells, α6-subunits form at least four different receptor subtypes composed as α6βxδ, α6α1βxδ, α6βγ2 and α6α1βγ2 (β isoform unspecified).[18]. Among them, the γ–containing receptors can form the two interfaces α+/γ- and α+/β-, which host the PQ binding sites of interest for potential therapeutic applications (see Figure 1).

While showing substantial promise *in vivo*,[19] the lead compounds show less than ideal properties. Metabolic stability and solubility are not ideal, the potency for the mPQ site is moderate, and residual activity in non– α6 receptors precludes use as truly selective research compounds.[20,21] One of the future synthetic aims thus is the introduction of groups that improve the biophysical properties. As a first step, we probed here the R7 position to establish its impact on the desired activity as PAM of α6β3γ2 receptors with a mini-library.

To improve data quality and mechanistic insight we selected concatenated receptors for the functional studies. Concatenation of the subunits of a pentameric protein like the $GABA_A$ receptor, by covalently linking the C-terminus of the preceding subunit with the *N*-terminus of the following subunit, offers the advantage of obtaining receptors with a defined stoichiometry and arrangement.[22] By combining appropriate triple and dual constructs we obtained four defined receptor configurations: two concatenated receptors, containing only one alpha isoform (α6β3α6γ2β3 and α1β3α1γ2β3), and two concatenated receptors containing two alpha isoforms (α6β3α1γ2β3 and γ2β3α1β3α6). Modulation of $GABA_A$ receptors resulting from expression of these constructs injected into *Xenopus laevis* oocytes by our compounds was then assessed by two–electrode voltage clamp technique.

Position 7 of the PQ scaffold proved to be a suitable position for the insertion of chemically different residues. This holds the potential for compounds with improved potency or selectivity compared to **2** or **3**, and could also serve as a convenient position to introduce residues that facilitate solubility,[20] or isotope based[23] or fluorescent labels to generate ligands useful for *in vitro* assays. We also discovered and describe differential interactions of our ligands with the α6+/γ2- interface.

2. Results

2.1. Chemistry

Pyrazoloquinolinones with eight different substituents in position R7 were synthesized and tested for their activity (Fig. 2). Compounds **1** and **2** have been described earlier.[24] Compounds **3, 4, 5, 6** were synthesized according to literature procedures as depicted in Scheme 1[25] starting from four different anilines a condensation with diethyl methylene malonate (**11a-d**) followed by a thermal cyclization yielded the oxo-quinolines **12a-d** in good yields. Upon the treatment of the oxo-quinolines with phosphoryl chloride the chloroquinolines **13a-d** were formed. The formation of the final pyrazoloquinolinones was performed using p-methoxy phenyl hydrazine hydrochloride in ethanol in the presence of triethylamine. The remaining PQs **7, 8, 9, 10** were synthesized as outlined in Scheme 2. Starting from compound **3** the TMS protected acetylene was introduced by a copper free Sonogashira coupling reaction which gave product **14** in relatively good yield. Compound **8** was obtained via deprotection with K_2CO_3. Reduction of the acetylene compound **8** under hydrogen atmosphere led to the ethyl derivative **9** in almost quantitative yields. For the hydration of the alkyne, which led to the formation of **10**, CF_3SO_3H was used as catalyst for the Markovnikov-type addition of water to the terminal alkyne at room temperature.[26]

2.2. Pharmacological results

2.2.1. Pharmacological characterization of receptors composed of loose or concatenated subunits

We have previously reported that the integration of the γ2 subunit is highly variable if *Xenopus laevis* oocytes are co–injected with mixtures of α6, β3 and γ2 mRNA[27] (Supplementary information ST1). Here we employed double (γ2β3) and triple (α6β3α6, α1β3α1, α6β3α1, α1β3α6) concatemers. They were prepared as described before[22,28,29] and appropriately co–injected into *Xenopus laevis* oocytes in order to form concatenated α6β3α6–γ2β3, α1β3α1–γ2β3, α6β3α1–γ2β3, and α1β3α6–γ2β3 receptors (Fig. 3). Two-electrode voltage-clamp studies were then performed in oocytes expressing either these concatenated receptors, or receptors resulting from injecting a mixture of individual α1 or α6/ β3/ γ2 subunit mRNA, henceforth referred to as loose α1–β3–γ2 or loose α6–β3–γ2 assemblies. Since the α1β3α6–γ2β3 receptor did not assemble well (see supplementary information SF1, ST2), it was redesigned with two different concatemers (double β3α6 and triple γ2β3α1) to form the newly arranged γ2β3α1–β3α6, still bearing

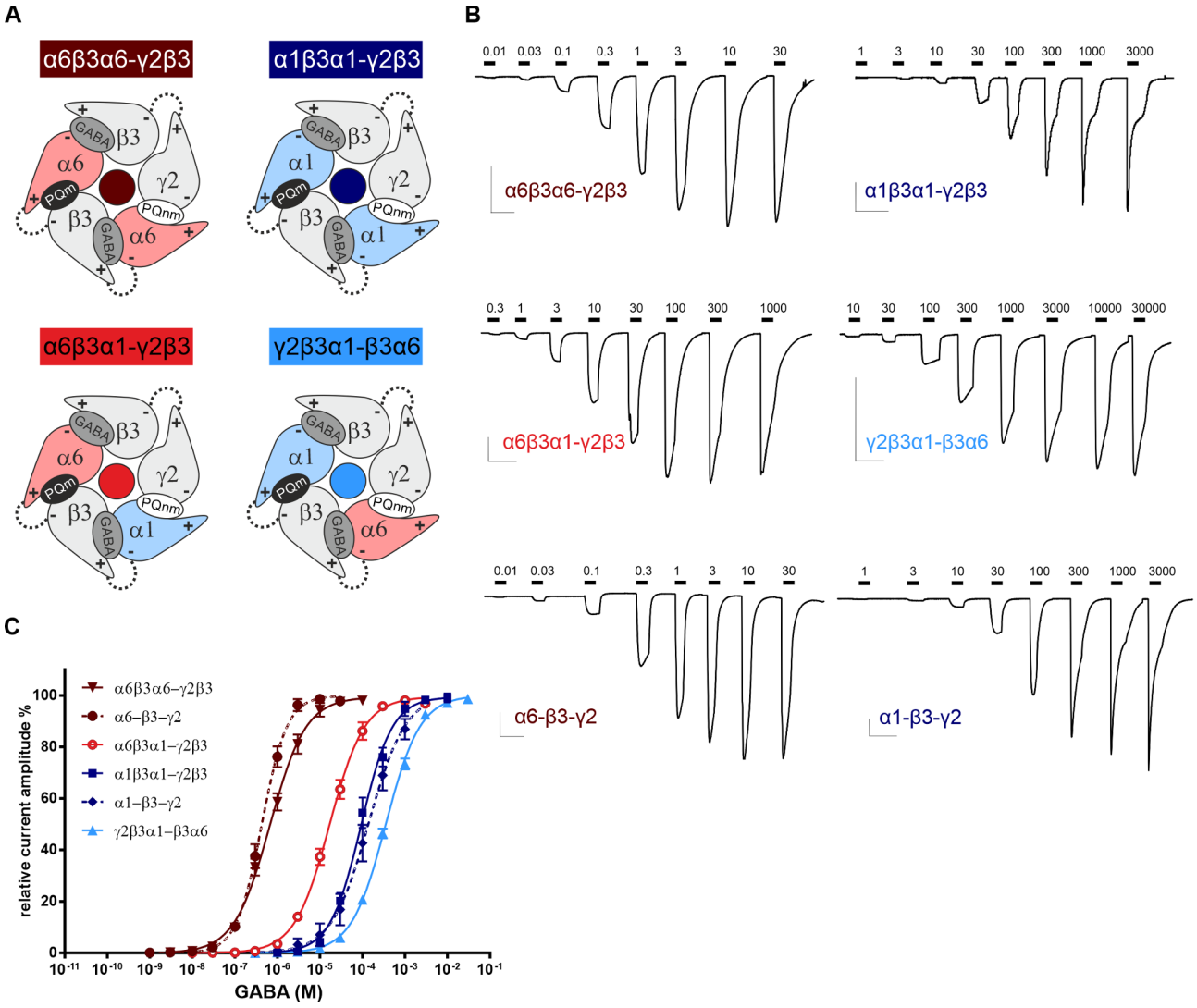

Figure 2. Structures of Pyrazoloquinolinones (PQs) used in this study. Compounds differ only in residue R7 (red).

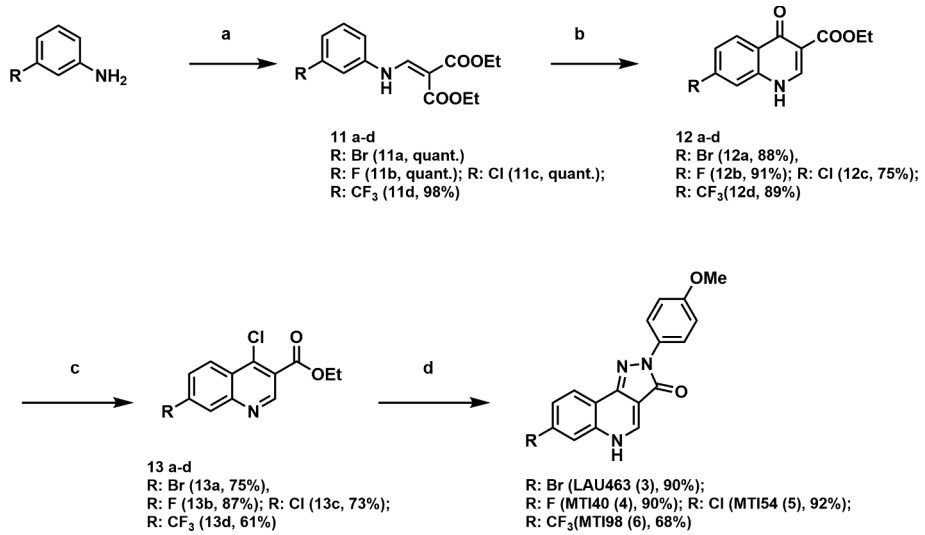

Scheme 1. a) diethyl(ethoxymethylene)malonate (1 equiv.), toluene, 110 °C, 24 h; b) diphenylether, 235 °C, 1 h; c) phosphoryl chloride (1 mL/mmol); 2 h, d) p-methoxy phenylhydrazine (1,1 equiv.), triethylamine (2.2 equiv.), ethanol, 24 h.

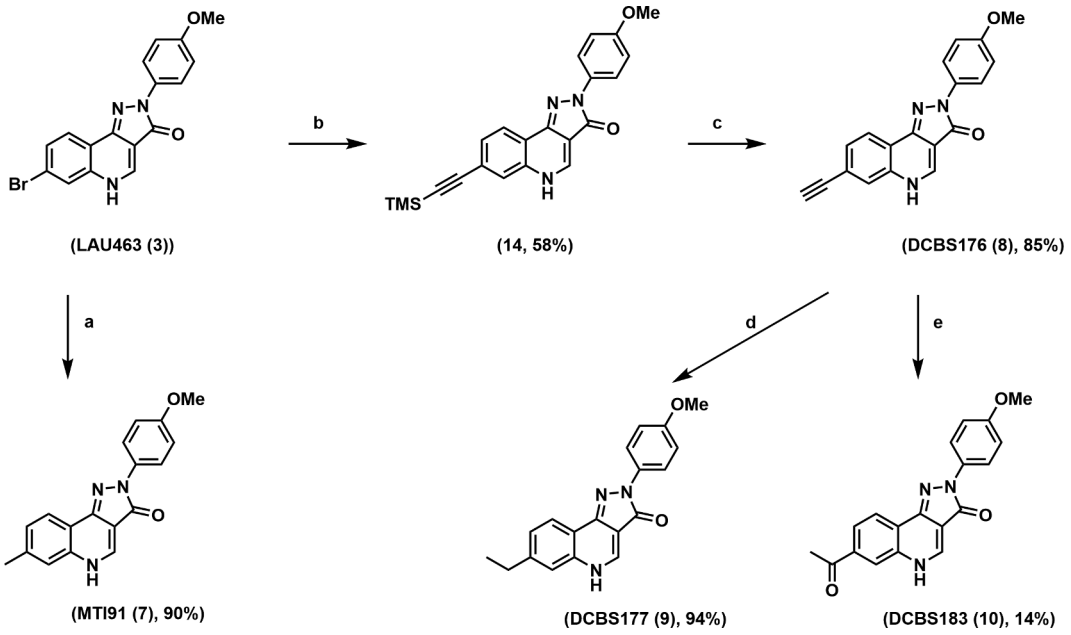

Scheme 2. a) Tetrakis(triphenylphosphine)palladium (0.1 equiv.), K_2CO_3 (2.5 equiv.), trimethylboroxine (1.5 equiv.), dioxane, 101 °C, 24 h; b) Palladium(II)acetate (0.1 equiv.), triphenylphosphine (0.2 equiv.), trimethylsilylacetylene (2 equiv), triethylamine/dimethylformamide (1:2), 100 °C, 17 h; c) K_2CO_3 (2 equiv.), methanol, rt, 2.5 h; d) Pd/C (10 wt%.), hydrogen, methanol, rt, 1 atm, 3.5 h; e) Trifluoromethylsulfonic acid (3.5 equiv.), water (2 equiv.), trifluoroethanol, 70 °C, 3d.

the same α1 + /β3- and α6 + /γ2- binding sites (Fig. 3).

In the three concatenated αxβ3αx–γ2β3 receptors the triple subunit concatemer αxβ3αx certainly forms one GABA–binding site at the β3 + /αx- and the PQm binding site at the αx + /β3- interface. If properly assembled, the second GABA binding site is then formed at the interface between the dual and the triple concatemer and the BZ/PQnm–site is formed between the triple and the dual concatemer (see Fig. 3A). In the alternative γ2β3α1–β3α6 concatenated conformation, the GABA sites are formed between β3 + /α1- and β3 + /α6-, while the PQm–site is formed between the triple and the double concatemer.

GABA concentration–response curves for all tested receptors are shown in Fig. 3B, C and Table 1. Comparison between concatenated receptors that contain only one alpha isoform (α1β3α1–γ2β3 and α6β3α6–γ2β3) and the corresponding loose subunit receptors (α1/α6–β3–γ2) revealed that the EC_{50} for GABA were similar (Table 1) in those cases where the GABA elicited currents were also comparable (supplementary table ST1 provides representative data for the much higher variability displayed by loose subunit combinations). Using a similar approach with the β2 isoform resulted in larger differences between the GABA EC_{50} for the comparison between non-concatenated and concatenated receptors.[22] The concatenated α6β3α1–γ2β3 receptors showed an intermediate apparent affinity between α1β3α1–γ2β3 and α6β3α6–γ2β3 concatenated receptors, but were closer to receptors containing α1 subunits. Conversely, the other concatenated receptor containing both α–isoforms γ2β3α1–β3α6 displayed the lowest apparent affinity.

Injection of the single (dimer and trimer) constructs served as control and none of the constructs alone produced considerable GABA currents (Table 1).

The positive allosteric modulator diazepam (DZ) acting at the BZ/PQnm binding site was used in order to check whether the triple and dual constructs had correctly assembled and formed the BZ/PQnm–site (Table 1). Receptors forming the α6 + /γ2- interface were insensitive to DZ, whereas receptors with the α1 + /γ2- interface responded with a positive modulation up to 250% at 1 μM DZ.

2.2.2. PQ effects in concatenated α6β3α6–γ2β3 $GABA_A$ receptors.

After having established that all four concatenated receptors were functional (Fig. 3, Table 1), we first tested the effects of the compounds in concatenated receptors containing only the α6–isoform. These should correspond to a defined recombinant version of native α6β3γ2 receptors.

In addition to the eight new analogues we also included the compounds PZII029 and CGS9895. All compounds were active in concatenated α6β3α6–γ2β3 receptors and positively modulated GABA–induced currents (Fig. 4, Table 2 and supplementary figure SF2, table ST3). Curves were reaching plateau values only for two compounds (LAU463, MTI54) at the highest tested dose of 30 μM (which is at the solubility limit). Three compounds (CGS9895, MTI91 and DCBS176) behaved similarly to known PQs tested in loose α6–β–γ2 receptors [10] and could be fitted by a classical monotonic sigmoid curve (Figure SF2 in supplement, Table ST3). Interestingly, dose responses to seven compounds (LAU463, PZII029, MTI98, DCBS177, DCBS183, MTI40, MTI54) were biphasic in concatenated α6β3α6–γ2β3 receptors, with a first component in the nanomolar range (EC_{50} ~ 10–50 nM) and the second in the micromolar range (EC_{50} ~ 20– 750 μM) (Fig. 4, and Table 2). This effect of PZII029 has been missed previously,[10] presumably because of the lower data quality that comes from a mixture of ternary and binary receptors in loose-subunit receptor expression (see also ST1).

2.2.3. Effects of LAU463 at low– and high–affinity binding sites.

In order to evaluate the involvement of the α6 + /γ2- binding site for PQ modulation, we further characterized LAU463 in the three remaining concatenated receptors.

PZII029 and LAU463 displayed the strongest modulation in the nM phase with an apparent EC_{50} of 8–9 nM. We decided to study LAU463 as the only compound whose curve reached plateau within the range of concentration that could be measured (Fig. 4B).

Concentration–response curves for LAU463 of all concatenated and loose receptor combinations are depicted in Fig. 5A–C. Respective data are reported in Table 3. Original traces are given in the supplementary information (SF 3).

Concatenated receptors containing either α6 or α1 alone responded similarly to respective loose subunit receptors to LAU463 (Fig. 5A). Concatenated receptors containing both α6 and α1 in two different positions within the receptor responded differently to LAU463 (Fig. 5B). When the BZ/PQnm–site was formed by α6 + /γ2- and the PQm–site by

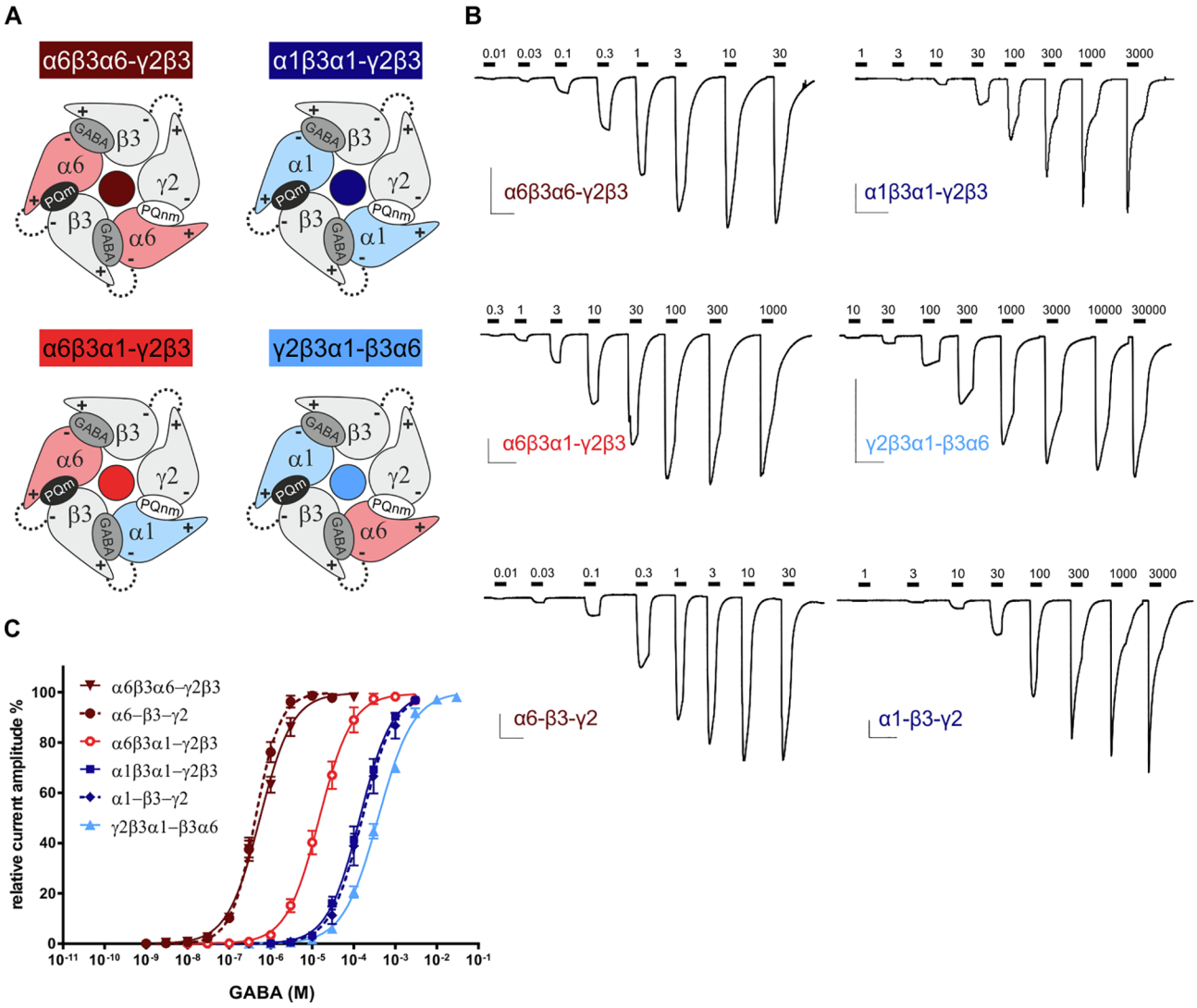

Figure 3. Concatenated receptors and their GABA responses. **A)** Schematic representation of the four concatenated receptors α6β3α6–γ2β3, α1β3α1–γ2β3, α6β3α1–γ2β3 and γ2β3α1–β3α6. Dotted lines indicate the linkers that form the concatenated subunits. **B)** Original traces of responses to GABA in concatenated and loose (α6–β3–γ2 or α1–β3–γ2) receptor combinations. Scale bars: 50 s/100nA **C)** GABA concentration–response curves. Individual curves were first normalized to the fitted maximal current and then averaged. Data represent mean ± SEM (n = 4–6) in at least two batches of oocytes.

Table 1
Effects of GABA and diazepam (DZ) in oocytes injected with concatenated or loose subunit cRNA. Fitted maximal GABA currents are given in nA. Single constructs generated negligible control currents. Current stimulation by 1 μM DZ is given in % of $EC_{1\text{-}1.5}$. Data represent mean ± SEM.

Concatenated constructs	GABA DR			GABA max	DZ 1 μM		
	EC_{50} (μM)	nH	n	current (nA)	potentiation (%)	(%)	n
α1β3α1-γ2β3	98 ± 15	1.3 ± 0.0	6	8050 ± 920	160		6
α6β3α6-γ2β3	0.7 ± 0.1	1.0 ± 0.1	5	2370 ± 250	0		9
α6β3α1-γ2β3	18 ± 2.5	1.1 ± 0.0	5	9350 ± 1700	250		5
γ2β3α1-β3α6	360 ± 27	1.0 ± 0.0	5	810 ± 230	0		5
α1β3α1	–	–	–	30 ± 2	–		3
α6β3α6	–	–	–	36 ± 19	–		5
α6β3α1	–	–	–	51 ± 18	–		4
γ2β3α1	–	–	–	69 ± 8	–		4
β3α6	–	–	–	0.5 ± 0.2	–		4
γ2β3	–	–	–	69 ± 3	–		3
Loose subunits							
α1-β3-γ2	160 ± 46	1.1 ± 0.1	5	13530 ± 7110	150		5
α6-β3-γ2	0.4 ± 0.0	1.5 ± 0.0	4	2650 ± 306	0		15

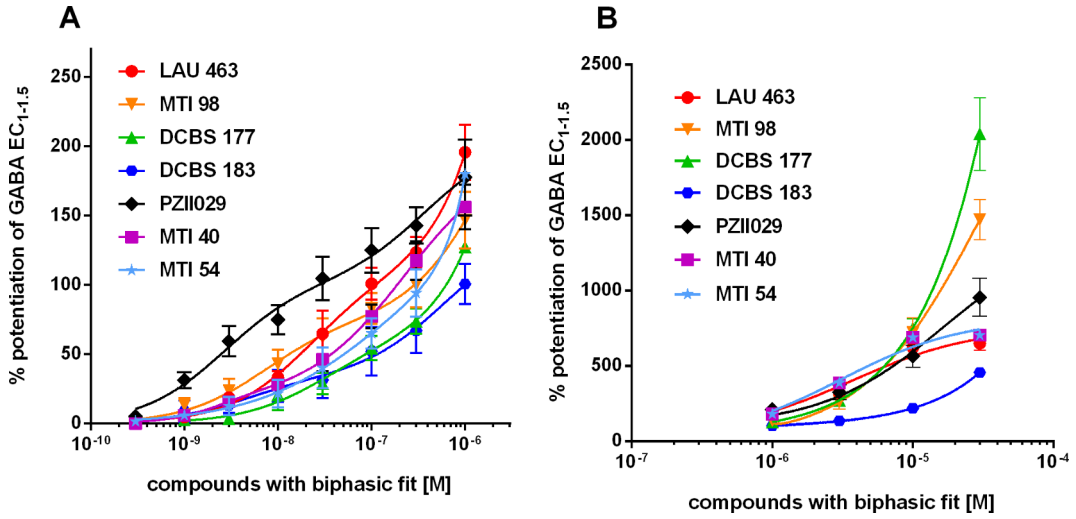

Figure 4. Concentration–response curves of tested compounds with a biphasic sigmoid behavior in concatenated α6β3α6–γ2β3 receptors. The first component is in the nanomolar range and the second in the micromolar range. **Panel A:** The first, more potent part of the dose–response curves until a compound concentration corresponding to 1 μM is displayed. **Panel B:** The second phase is displayed. Both panels: Control current = 0% (GABA $EC_{1\text{-}1.5}$). For complete efficacy data see supplementary table ST4. Data represent mean ± SEM (n = 4–7).

Table 2
EC_{50}, Hillslopes (nH) and fitted maximal currents (Top %) of tested biphasic compounds at increasing concentrations in concatenated α6β3α6-γ2β3 receptors. Parameters of the more potent first phase are indicated with A (nM), of the second less potent phase with B (μM). Data are reported as mean ± SEM in at least two batches of oocytes. Control current = 0% (GABA $EC_{1\text{-}1.5}$).

α6β3α6-γ2β3	LAU 463	PZII029	MTI 98	DCBS 177
Top (A) (%)	82 ± 24	113 ± 18	49 ± 12	57 ± 9
EC_{50} (A) (nM)	9 ± 2	8 ± 3	13 ± 5	23 ± 5
nH (A)	= 1.0	= 1.0	= 1.0	= 1.0
Top (B) (%)	657 ± 38	1628 ± 228	2972 ± 301	4984 ± 398
EC_{50} (B) (μM)	24 ± 7	118 ± 32	100 ± 4	299 ± 34
nH (B)	=1.0	=1.0	=1.0	=1.0
n	7	5	5	5
α6β3α6-γ2β3	DCBS 183	MTI 40	MTI 54	
Top (A) (%)	82 ± 17	96 ± 11	56 ± 23	
EC_{50} (A) (nM)	50 ± 8	28 ± 10	10 ± 2	
nH (A)	=1.0	=1.0	=1.0	
Top (B) (%)	2210 ± 298	353 ± 25	796 ± 44	
EC_{50} (B) (μM)	735 ± 212	32 ± 11	17 ± 4	
nH (B)	=1.0	=1.0	=1.0	
n	5	6	4	

α1+/β3-, LAU463 positively modulated currents at nM and μM concentrations, producing a biphasic curve. 100 nM elicited approximately 40% potentiation, and maximal efficacy at 30 μM reached about 200% potentiation. Conversely, when the BZ/PQnm–site was formed by α1+/γ2- and the PQm–site by α6+/β3-, LAU463 activated the receptors in a monophasic way, with no modulation at low concentrations and a potentiation of 1000% at 30 μM.

A closer look at the first high affinity phase of LAU463 (Fig. 5C) revealed that the γ2β3α1–β3α6 receptor clearly responded to lower doses of LAU463 compared to the opposite alpha subunit arrangement α6β3α1–γ2β3, although it did not reach the same potentiation as α6β3α6–γ2β3 receptors (50% at 30 nM).

Taken together, these results show that LAU463 does not only discern between α6+ and α1+ at the low affinity PQm site, but also at the high affinity BZ/PQnm site.

2.2.4. Effects of R7 substitution on the mPQ effect

After having established the source of the high affinity modulation of LAU463, we analyzed the impact of the different R7 groups on the strong modulation exerted by the mPQ site at the α+/β3- interface for the α1 and α6 isoforms. All compounds tested here elicited robust modulation of the α6β3α6–γ2β3 receptor in the micromolar phase (Fig. 4, supplementary figure SF2, supplementary tables ST3, ST4). The apparent potency as assessed by the EC_{50} values ranged from ~20 nM (LAU463) to > 100 μM. To assess functional selectivity for α6+/β3- over α1+/β3-, we tested several compounds in the α1β3α1–γ2β3 receptor and found DCBS183 to be nearly inactive (only ~10% modulation, see supplementary table ST 7). Further experiments will be required to obtain complete selectivity profiles of the most promising compounds obtained in this study and additional derivatives that may feature better potency compared to LAU463 and similar selectivity as DCBS183.

2.3. Structural analysis of the ECD pocket of the tested alpha subunits

Recently released cryo-EM structures[5,30] allow the visualization of the extracellular pocket of interest and to analyze potential determinants of (functional) α6- selectivity. We depict the principal part of the ECD pocket in Fig. 6 and provide an overview of the conserved and variable positions across the alpha isoforms.

Generally, $GABA_A$ receptor subunits possess high sequence identity and high sequence similarity. At the ECD α+/β- interfaces, unique amino acid residues define the binding pockets. Alpha subunit isoforms have been placed according to pharmacological similarities into groups: the diazepam-sensitive (α 1, 2, 3, 5) and the diazepam-insensitive subunits (α 4,6) differ in loop A,[2] while loop B contributes to zolpidem sensitive subunits (α 1, 2, 3) and the zolpidem insensitive[31] group (α 4, 5, 6) As shown in Fig. 6 it is possible to divide the amino acids at the interface into the conserved group (conserved among all the alpha subunits; graphically depicted as yellow spheres in panel 6C) and variable among the isoforms (orange spheres). Amino acids that contribute to the extracellular binding pocket are marked with a green asterisk. The major difference between the α1 and α6 subunits in loop A is the presence of a histidine (H) and arginine (R) respectively. The threonine residue (T) on the loop B of α1 corresponds to a proline (P) in α6. Most differences are found in loop C, which is the least conserved and gives each alpha isoform its unique selectivity profile.

Thus, the combined features of so- called loops A, B and C give each alpha isoform a completely unique ligand recognition principal surface. The α6 and α1 subunits differ in a total of five pocket forming positions from one another, one on loop A that confers diazepam insensitivity to α6, one in loop B that confers zolpidem insensitivity to α6 and three

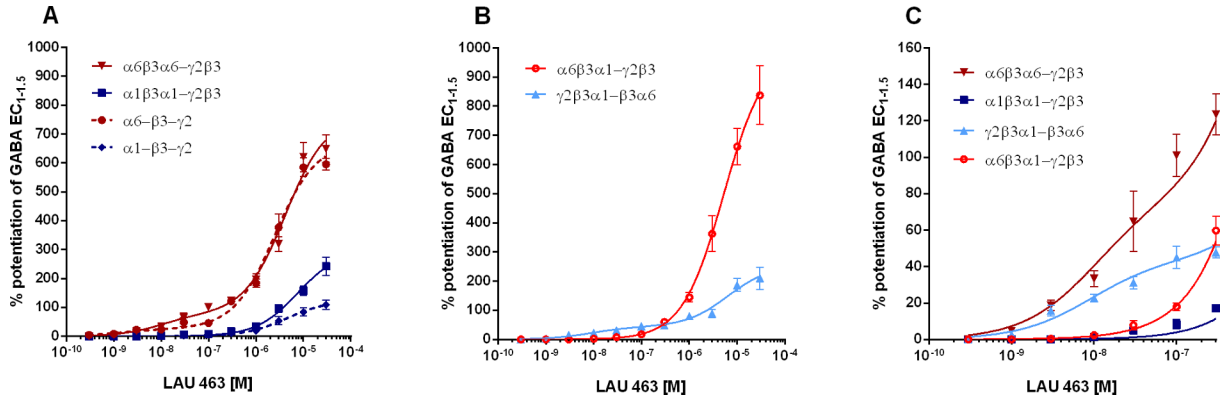

Figure 5. Effects of LAU463 in different concatenated and loose receptors. **A)** Concatenated receptors containing only the subunit isoform α6 or α1 (continuous lines) responded similarly to respective loose subunit receptors (dotted lines). Reduced efficacy in loose subunit receptors possibly reflects the heterogeneity of the receptor population (binary and ternary receptors) **B)** Concatenated receptors containing both α–subunit isoforms α6β3α1–γ2β3 and γ2β3α1–β3α6 responded differently to LAU463: null modulation at the α1 + /γ2- site and high positive modulation at the α6 + /β3- site (red curve) vs. little modulation at the α6 + /γ2- site and reduced positive modulation at the α1 + /β3- site (light blue curve). **C)** Enlarged view of the high affinity phase of LAU463 in all concatenated receptors: γ2β3α1–β3α6 receptors responded already to lower doses of LAU463 compared to α6β3α1–γ2β3 receptors. Data represent mean ± SEM (n = 4–7). Control current = 0% (GABA $EC_{1\text{-}1.5}$).

positions on loop C. All these positions could contribute potentially to binding selectivity, as well as to the so-called functional selectivity. The latter can also be influenced by non-local sequence differences.[32]

3. Discussion

Receptors containing the α6 subunit are expressed both in the central and in the peripheral nervous system.[16,33] Their relevance as potential drug targets is supported by studies in which involvement of these receptors in motor tic disorders, orofacial and temporomandibular joint pain, and some symptoms of depression has been suggested.[15,17,19,27]

The PQ derivatives PZII029 (Ŕ4 and R7 = methoxy), and LAU463 (Ŕ4 = methoxy and R7 = bromo) were presented as first functionally selective α6β3γ2 ligands.[9,10] As the position 7 seems to be at least partly responsible for the high efficacy at the desired α6β3γ2 receptor subtype, modifications at this position have been investigated here with the introduction of chemically diverse substituents. Different halogens as well as substituents with or without "functionality" were explored (Fig. 4). All substituents led at high concentration to activity in α6β3α6γ2 receptors similar to the one observed for PZII029 and LAU463.

Over the whole concentration range, we observed a nM modulatory component for seven of the compounds. This was explored mechanistically for LAU463 by taking advantage of concatenated receptor as described previously.[34] Using mixed concatenated receptors that feature either the α6/γ2 interface together with α1/β3, or the α6/β3 interface together with α1/γ2, we were able to attribute the high affinity effect elicited by LAU463 to the α6/γ2 interface and the low affinity effect to the α6/β3 interface. Thanks to the forced subunit assembly obtained by the use of concatenated receptors, we were thus able to observe a positive modulation of GABA–induced currents that is ascribable to individual interfaces. Since at least three PQ binding sites have been proposed so far,[6,8,35] this approach provides valuable insights into the functional effects mediated by individual binding sites. Some PQs have been suggested that interact with the TMD sites,[8] but the majority of the modulatory action appears to be elicited by the ECD.[32] As additional advantage, site directed mutagenesis could also be employed in order to modify individual subunits and one binding site at a time. The efficacy of the tested PQs in the nM–phase is highest when methoxy (followed by Br) is the substituent in position R7, but beyond this observation, no SAR hints can be extracted from the data.

The low affinity modulation is very similar for all tested compounds, both in potency as well as in efficacy. This indicates that the R7 position is remarkably tolerant to a wide range of substituents, and therefore may be well suited to introduce functionality compounds without loss of activity. Furthermore, R7 can serve as site of introduction for isotope labelled group to facilitate detection,[23] or covalently reactive groups to label receptors in ex vivo samples, or possibly even to improve "druggability" of the PQ scaffold.[20]

Conclusions about the structural correlates for the subtype difference in efficacy in the pockets can only be speculative at the current state of research. The two alpha isoforms used here differ in all three principal loops (Fig. 6). While the contributions of loops A and B to diazepam- and zolpidem sensitivity have been described, the determinants of so-called "functional selectivity" are less well understood. Loop C features three differences in pocket lining positions, and two more in positions that may impact on loop C geometry in indirect ways. Any of

Table 3
EC_{50}, Hillslopes (nH) and fitted maximal currents (Top %) of LAU463 at increasing concentrations in concatenated α6β3α6–γ2β3, γ2β3α1–β3α6, α1β3α1–γ2β3, α6β3α1–γ2β3 or loose α6 –β3–γ2 and α1–β3–γ2 receptors. Receptors required either a monotonic sigmoid or biphasic fit. Parameters of the high affinity (or first) phase are indicated with A, of the micromolar phase with B). For complete efficacy data see supplementary table ST5. Control current = 0% (GABA $EC_{1\text{-}1.5}$). Data are reported as mean ± SEM.

LAU 463	α1β3α1-γ2β3	α1-β3-γ2	γ2β3α1-β3α6	α6-β3-γ2	α6β3α1-γ2β3
Top (A) (%)			30 ± 7	70 ± 16	
EC_{50} (A) (nM)			4 ± 4	1 ± 0.1	
nH (A)			=1.0	=1.0	
Top (B) (%)	342 ± 25	132 ± 10	230 ± 22	580 ± 26	1060 ± 51
EC_{50} (B) (μM)	10 ± 2	6 ± 1	36 ± 15	11 ± 2	7 ± 0.1
nH (B)	=1.0	=1.0	=1.0	=1.0	=1.0
n	7	6	6	6	7

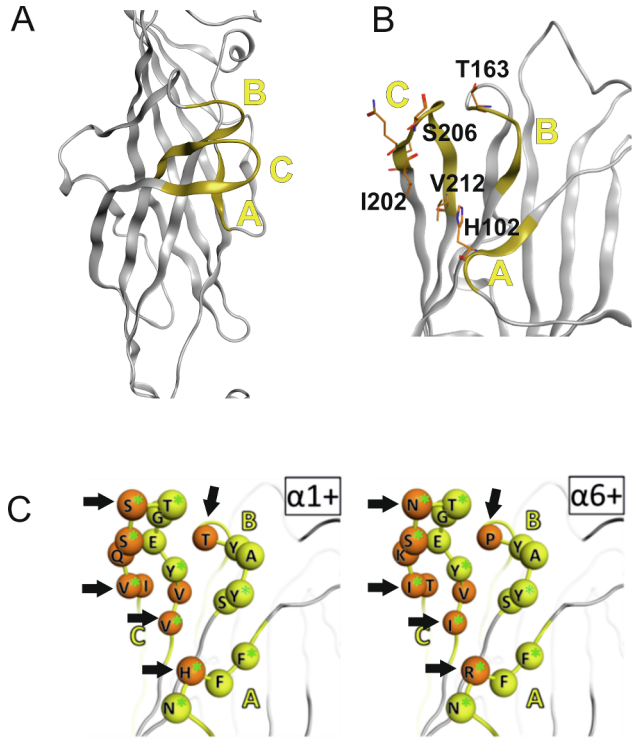

Figure 6. Comparison between the principal pocket part (plus side) between α1 and an α6 model: **A)** Overview of the ECD of an α1 subunit from 6D6T[30], loops A, B, C in yellow ribbon. **B)** View of the subunit turned to offer a look "into" the half-pocket that is made up by loops A, B and C. Amino acids that contribute in 6D6T to the benzodiazepine pocket and are different from their homologues in the α6 subunit are shown in stick representation, and those which contribute to the pocket are identified with the numbering as in 6D6T (human protein without signal peptide). The detailed comparison in the next panel depicts the loops in the same orientation. **C)** Extracellular plus sides of α1 and α6 (model) in comparison, showing amino acid positions that are conserved (yellow) and non-conserved (orange) among all six alpha isoforms. Green asterisks denote amino acids whose sidechains point towards the pocket. Orange CA atoms denote positions where the alpha isoforms show sequence differences. Black arrows point to those positions where sidechains contribute to the pocket, and in which α1 and α6 differ.

these could impact on the observed modulatory responses that mainly differ in efficacy. In addition, non-local effects could also contribute to efficacy. The structural analysis guides the path forward to systematic mutational analysis for the pocket determinants that could be targeted specifically to improve both potency and efficacy selective modulation.

4. Conclusions

All together we have confirmed that defined concatenated receptors are highly useful to conduct mechanistic studies. We were able to define an interesting additive dual mode of action of some R7 substituted PQs.

Compounds that can discern between α6 + /γ2- and α1 + /γ2- at the BZ/PQnm–binding site would be of great interest as a valuable tool compound for biochemical studies of brain regions where mixed $GABA_A$ receptors containing the alpha isoforms α1 and α6 together with β/γ subunits are involved.[18] Additionally, such compounds may be helpful for oocyte electrophysiology in labs that inject loose $GABA_A$ subunits instead of concatenated $GABA_A$ receptors, in order to check for correct receptor assembly. However, the compounds presented here are not yet well suited for these purposes due to their low efficacy at the high affinity phase.

Nevertheless, subunit concatenation is the first choice for studies in oocytes because it abolishes or at least minimizes the formation of undesired receptor arrangements and allows detecting and attributing even fairly small compound effects to defined interfaces within the receptor.

Moreover, we demonstrated the suitability of R7 as convenient entry point for chemical diversity of PQs without concomitant loss of activity at their high efficacy modulatory site. The R7 position is also seemingly suitable to improve the selectivity of the compounds, but showed only marginal potential to improve potency for the mPQ site.

5. Experimental

5.1. Chemistry

5.1.1. General

All reactions were performed in oven-dried round-bottom flasks with magnetic stir bars or overhead mechanical stirrers under an argon atmosphere unless the reaction conditions were supposed to contain water. Organic solvents were purified when necessary by standard methods or purchased from Sigma-Aldrich.™ Chemicals were purchased from either Sigma AldrichTM, Oakwood Chemical, Alfa Aesar, Matrix Scientific, or Acros Organic. Commercially available reagents were used without further purification. Reactions were monitored by thin layer chromatography with silica gel 60 F_{254} plates (E. Merck, Darmstadt, Germany). For chromatography separation Light petroleum (LP) with a boiling point range of 40–60 °C was used. HPLC chromatography was carried out with the Autopurification system by Waters using fluoro-phenyl columns. ^1H and ^{13}C NMR spectra were recorded on Bruker Avance Ultrashield 400 (^1H: 400 MHz, ^{13}C: 101 MHz). Chemical shifts are reported in parts per million (ppm) and were calibrated using DMSO-d_6 as internal standard. Multiplicities are denoted by s (singlet), br s (broad singlet), d (doublet), dd (doublet of doublet) and m (multiplet). Melting points were determined with a Büchi Melting Point B-545 apparatus. HR-MS was measured on an Agilent 6230 LC TOFMS mass spectrometer equipped with an Agilent Dual AJS ESI-Source.

5.1.2. General procedure A: Synthesis of compounds **11 a-d**

1 equiv. of diethyl(ethoxymethylene)malonate was added to a solution of the substituted aniline in toluene (1.25 mL/mmol) and the reaction mixture was heated to reflux for 24 h. After the full consumption of the starting material the solvent was removed under reduced pressure and the product was purified via column chromatography (gradient of 10%-30% EtOAc in LP).

*5.1.2.1. Diethyl 2-(((3-bromophenyl)amino)methylene)malonate (**11a**).* Malonate **11a** (colorless solid, 9.9 g, quant.) was obtained from 3-bromoaniline (5.03 g, 29 mmol) and diethyl(ethoxymethylene)malonate (6.27 g, 29 mmol) according to general procedure A; m.p. 71–73 °C; ^1H NMR (400 MHz, $CDCl_3$) δ 1.33 (t, J = 7.1 Hz, 3H), 1.37 (t, J = 7.1 Hz, 3H), 4.25 (q, J = 7.1 Hz, 2H), 4.30 (q, J = 7.1 Hz, 2H), 7.02 – 7.06 (m, 1H), 7.19 – 7.30 (m, 3H), 8.44 (d, J = 13.4 Hz, 1H), 10.98 (br d, J = 13.5 Hz, 1H); ^{13}C NMR (101 MHz, $CDCl_3$) δ 14.4, 14.5, 60.4, 60.7, 94.8, 115, 120.2, 123.7, 127.8, 131.2, 140.7, 151.3, 165.6, 169.0.

*5.1.2.2. Diethyl 2-(((3-fluorophenyl)amino)methylene)malonate (**11b**).* Malonate **11b** (colorless solid, 2.5 g, quant.) was obtained from 3-fluoroaniline (1 g, 9 mmol) and diethyl(ethoxymethylene)malonate (1.95 g, 9 mmol) according to general procedure A; m.p. 49 °C; ^1H NMR (200 MHz, *d*-DMSO) δ 1.26 (td, J = 7.1, 6.1 Hz, 6H), 4.13 (q, J = 7.1 Hz, 2H), 4.21 (q, J = 7.1 Hz, 2H), 6.97 (tdd, J = 8.5, 2.5, 0.8 Hz, 1H), 7.22 (ddd, J = 8.3, 2.2, 0.9 Hz, 1H), 7.33 – 7.47 (m, 2H), 8.38 (d, J = 13.7 Hz, 1H), 10.67 (d, J = 13.7 Hz, 1H); ^{13}C NMR (50 MHz, *d*-DMSO) δ 14.6 , 14.7, 60.1, 60.3, 94.7, 105.4 (d, $^2J_{C,F}$ = 25.9 Hz,), 111.4 (d, $^2J_{C,F}$ = 21.2 Hz), 114.0 (d, $^4J_{C,F}$ = 2.8 Hz), 131.8 (d, $^3J_{C,F}$ = 9.6 Hz), 141.8 (d, $^3J_{C,F}$ = 10.6 Hz), 151.1, 163.3 (d, $^1J_{C,F}$ = 243.1 Hz), 165.3, 167.5.

*5.1.2.3. Diethyl 2-(((3-chlorophenyl)amino)methylene)malonate (**11c**).* Malonate **11c** (colorless solid, 2.3 g, quant.) was obtained from 3-chloroaniline (1 g, 7.8 mmol) and diethyl(ethoxymethylene)malonate (1.69 g, 7.8 mmol) according to general procedure A; m.p. 53–56 °C; ^{1}H NMR (200 MHz, *d*-DMSO) δ 1.25 (q, J = 7.0 Hz, 6H), 4.13 (q, J = 7.1 Hz, 2H), 4.22 (q, J = 7.1 Hz, 2H), 7.19 (ddd, J = 7.7, 2.0, 1.2 Hz, 1H), 7.25 – 7.45 (m, 2H), 7.56 (t, J = 2.0 Hz, 1H), 8.36 (d, J = 13.7 Hz, 1H), 10.63 (d, J = 13.7 Hz, 1H); ^{13}C NMR (50 MHz, *d*-DMSO) δ 14.2,59.7, 94.4, 116.2, 117.7, 124.2, 131.2, 134.0, 141.1, 150.7, 164.9, 167.0.

*5.1.2.4. Diethyl 2-(((3-(trifluoromethyl)phenyl)amino)methylene)malonate (**11d**).* Malonate **11d** (colorless solid, 1 g, 98%.) was obtained from 3-trifluoromethylaniline (500 mg, 3.1 mmol) and diethyl (ethoxymethylene)malonate (670 mg, 3.1 mmol) according to general procedure A; m.p. 46 °C; ^{1}H NMR (400 MHz, DMSO-d_6) δ 1.25 (t, J = 7.1, 7.1 Hz, 6H), 4.18 (s, 4H), 7.47 (ddt, J = 7.7, 1.8, 0.9, 0.9 Hz), 7.60 (td, J = 7.9, 7.6, 0.9 Hz, 1H), 7.69 (dd, J = 8.1, 2.3 Hz, 1H), 7.79 – 7.84 (m, 1H), 8.41 (s, 1H), 10.72 (s, 1H); ^{13}C NMR (101 MHz, *d*-DMSO) δ 14.7, 60.2, 95.2, 115.2 (q, $^2J_{C,F}$ = 4.1 Hz), 121.1 (q, $^3J_{C,F}$ = 4.1 Hz), 121.6, 124.1 (q, $^1J_{C,F}$ = 271.6 Hz), 130.7 (q, $^2J_{C,F}$ = 32.1 Hz), 131.2, 140.9, 151.1.

*5.1.3. General procedure B: Synthesis of compounds **12 a-d***

The malonate derivates **11a-d** were dispersed in diphenylether (1.7 mL/mmol), flushed with argon and heated to 235 °C for 1 h with a heating jacket. The reaction mixture was poured into petroleum ether, the formed precipitate was collected by filtration and washed with a mixture of LP/EtOAc 1/1 to yield the desired product.

*5.1.3.1. Ethyl 7-bromo-4-oxo-1,4-dihydroquinoline-3-carboxylate (**12a**).* **12a** (colorless solid, 5 g, 88%) was obtained from **11a** (5.03 g, 29 mmol) according to general procedure B; m.p. > 300 °C; ^{1}H NMR (600 MHz, DMSO-d_6) δ 1.27 (t, J = 7.1 Hz, 3H), 4.21 (q, J = 7.1 Hz, 2H), 7.57 (dd, J = 8.6, 1.9 Hz, 1H), 7.82 (d, J = 1.9 Hz, 1H), 8.06 (d, J = 8.6 Hz, 1H), 8.58 (s, 1H), 12.31 (s, 1H); ^{13}C NMR (151 MHz, DMSO-d_6) δ 14.8, 60.2, 110.9, 121.5, 126.2, 126.6, 128.2, 128.4, 140.5, 146.0, 165.0, 173.3.

*5.1.3.2. Ethyl 7-Fluoro-4-oxo-1,4-dihydroquinoline-3-carboxylate (**12b**).* **12b** (colorless solid, 1.55 g, 91%.) was obtained from **11b** (5.03 g, 29 mmol) according to general procedure B; m.p. > 300 °C; ^{1}H NMR (400 MHz, DMSO-d_6) δ 1.27 (t, J = 7.1 Hz, 3H), 4.21 (q, J = 7.1 Hz, 2H), 7.27 (td, J = 8.8, 2.4 Hz, 1H), 7.38 (dd, J = 9.8, 2.5 Hz, 1H), 8.20 (dd, J = 9.0, 6.3 Hz, 1H), 8.57 (s, 1H), 12.30 (s, 1H); ^{13}C NMR (151 MHz, DMSO-d_6) δ 14.8, 60.1, 104.7 (d, $^2J_{C,F}$ = 25.2 Hz), 110.7, 113.7 (d, $^2J_{C,F}$ = 23.4 Hz), 124.7, 129.5 (d, $^3J_{C,F}$ = 10.9 Hz), 140.9, 146.1, 164.5 (d, $^1J_{C,F}$ = 249.2 Hz), 165.1, 173.2.

*5.1.3.3. Ethyl 7-Chloro-4-oxo-1,4-dihydroquinoline-3-carboxylate (**12c**).* **12c** (colorless solid, 2.4 g, 75%.) was obtained from **11c** (3.7 g, 12.4 mmol) according to general procedure B; m.p. decomposition > 325 °C; ^{1}H NMR (400 MHz, DMSO-d_6) δ 1.28 (t, J = 7.1 Hz, 3H), 4.22 (q, J = 7.1 Hz, 2H), 7.45 (dd, J = 8.7, 2.0 Hz, 1H), 7.68 (d, J = 2.0 Hz, 1H), 8.14 (d, J = 8.7 Hz, 1H), 8.60 (s, 1H), 12.33 (s, 1H); ^{13}C NMR (101 MHz, DMSO-d_6) δ 14.3, 59.7, 110.5, 118.1, 125.0, 125.9, 128.0, 136.9, 139.9, 145.6, 164.6, 172.8.

5.1.3.3 Ethyl 7-trifluoromethyl-4-oxo-1,4-dihydroquinoline-3-carboxylate (**12d**)

12d (colorless solid, mixture of keto and enol form 3: 1, 2.4 g, 89%.) was obtained from **11d** (3.7 g, 12.4 mmol) according to general procedure B; m.p. 295–297 °C; ^{1}H NMR (400 MHz, DMSO) Keto-form: δ 1.29 (t, J = 7.1 Hz, 3H), 4.17 – 4.28 (m, 2H), 7.71 (d, J = 8.5 Hz, 1H), 7.99 (s, 1H), 8.34 (d, 1H), 8.70 (s, 1H), 12.50 (s, 1H); Enol-form: δ 1.29 (t, J = 7.1 Hz, 3H), 4.17 – 4.28 (m, 2H), 7.78 – 7.85 (m, 1H), 7.87 – 7.92 (m, 1H), 8.53 (s, 1H).

^{13}C NMR not recorded for solubility issues

*5.1.4. General procedure C: Synthesis of compounds **13a-d***

The quinoline derivate was dispersed in $POCl_3$ (1 mL/mmol) and heated to reflux. After 2 h the reaction mixture was poured onto ice, neutralized with satd. $NaHCO_3$, extracted with CH_2Cl_2 (3 × 12 mL/mmol), washed with brine (1 × 12 mL/mmol), dried over Na_2SO_4, filtered and evaporated. The residue was purified by FC (gradient of 5%-15% EtOAc in LP to give the desired product.

*5.1.4.1. Ethyl 7-bromo-4-chloroquinoline-3-carboxylate (**13a**).* The chloro quinoline **13a** (colorless solid, 400 mg, 75%) was obtained from **12a** (500 mg, 1.7 mmol) according to general procedure C; m.p. 91–92 °C; ^{1}H NMR (400 MHz, DMSO-d_6) δ 1.38 (t, J = 7.1 Hz, 3H), 4.43 (q, J = 7.1 Hz, 2H), 8.00 (dd, J = 9.0, 2.0 Hz, 1H), 8.30 (dd, J = 9.0,1H), 8.39 (d, J = 2 Hz, 1H), 9.17 (s, 1H); ^{13}C NMR (101 MHz, DMSO-d_6) δ 14.0, 62.1, 123.6, 124.3, 126.2, 127.1, 131.4, 132.2, 141.9 , 149.3, 150.9, 163.6.

*5.1.4.2. Ethyl 7-fluoro-4-chloroquinoline-3-carboxylate (**13b**).* The chloro quinoline **13b** (colorless solid, 400 mg, 87%) was obtained from **12b** (500 mg, 1.8 mmol) according to general procedure C; m.p. 59–62 °C; ^{1}H NMR (400 MHz, DMSO-d_6) δ 1.27 (t, J = 7.1 Hz, 3H), 4.22 (t, J = 7.1 Hz, 2H), 7.27 (td, J = 8.8, 2.5 Hz, 1H), 7.43 (dd, J = 9.9, 2.5 Hz, 1H), 8.19 (dd, J = 9.0, 6.3 Hz, 1H), 8.56 (s, 1H); ^{13}C NMR (101 MHz, DMSO-d_6) δ 14.2, 62.2, 113.7 (d, $^2J_{C,F}$ = 20.9 Hz), 118.9 (d, $^2J_{C,F}$ = 25.3 Hz), 122.5, 123.3, 128.1 (d, $^3J_{C,F}$ = 10.2 Hz), 143.6, 150.8, 151.4, 164.2, 164.4 (d, $^1J_{C,F}$ = 162.9 Hz).

*5.1.4.3. Ethyl 7-chloro-4-chloroquinoline-3-carboxylate (**13c**).* The chloro quinoline **13c** (colorless solid, 550 mg, 73%) was obtained from **12b** (700 mg, 2.8 mmol) according to general procedure C; m.p. 82–84 °C; ^{1}H NMR (DMSO, 400 MHz): δ 1.27 (t, J = 7.1 Hz, 3H), 4.21 (q, J = 7.1 Hz, 2H), 7.44 (dd, J = 8.7, 2.0 Hz, 1H), 7.72 (d, J = 2.0 Hz, 1H), 8.13 (d, J = 8.6 Hz, 1H), 8.57 (s, 1H); ^{13}C NMR ($CDCl_3$, 50 MHz):δ 14.4 (q, CH3), 62.3, 123.2, 124.8, 127.0, 128.9, 129.5, 138.4, 143.7, 150.0, 151.5, 164.3.

*5.1.4.4. Ethyl 7-trifluoromethyl-4-chloroquinoline-3-carboxylate (**13d**).* The chloro quinoline **13d** (colorless solid, 260 mg, 61%) was obtained from **12d** (400 mg, 1.4 mmol) according to general procedure C; m.p. 82–84 °C; ^{1}H NMR (400 MHz, $CDCl_3$) δ 1.48 (t, J = 7.1 Hz, 3H), 4.52 (q, J = 7.1 Hz, 2H), 7.87 (dd, J = 8.9, 1.8 Hz, 1H, H6), 8.39 – 8.50 (m, 1H), 8.54 (dt, J = 8.9, 0.8 Hz, 1H), 9.28 (s, 1H); ^{13}C NMR (101 MHz, $CDCl_3$) δ 14.2, 62.4, 123.4 (q, $^1J_{C,F}$ = 272.8 Hz), 124.0 (q, $^3J_{C,F}$ = 3.2 Hz), 124.7, 126.9, 127.7 (q, $^3J_{C,F}$ = 4.3 Hz), 127.8, 133.5 (q, $^2J_{C,F}$ = 33.2 Hz), 143.4, 148.6, 151.4, 164.0.

*5.1.5. General procedure D: Synthesis of Pyrazoloquinolinones (**3–10, 14**)*

The chloro quinoline (1 equiv.) and the p-methoxy phenyl hydrazine hydrochloride (1.1 equiv.) were dispersed in EtOH (4 mL/mmol), Et_3N (2.2 equiv.) was added and the reaction mixture was heated to reflux under argon atmosphere. After 20 h the reaction mixture was rinsed with water (2 mL/mmol), filtered and the precipitate was washed with EtOAc/LP (1/1) (20 mL/mmol). The residue was dried under reduced pressure to give the desired product. Purification by HPLC was applied if specified.

*5.1.5.1. 7-Bromo-2-(4-methoxyphenyl)-2,5-dihydro-3H-pyrazolo[4,3-c] quinolin-3-one (**3**).* PQ **3** (yellow solid, 2.5 g, 90%) was obtained from **13a** (2.4 g, 7.62 mmol) according to general procedure D; m.p. decomposition > 300 °C; ^{1}H NMR (400 MHz, DMSO-d_6) δ 3.78 (s, 3H, OCH_3), 7.01 (d, J = 9.2 Hz, 2H, H3′ and H5′), 7.69 (dd, J = 10.1, 2.0 Hz, 1H, H8), 7.88 (d, J = 1.9 Hz, 1H), 8.06 (d, J = 9.2 Hz, 2H), 8.13 (d, J = 8.6 Hz, 1H), 8.74 (s, 1H), 12.80 (br s, 1H); ^{13}C NMR (101 MHz, DMSO-d_6) δ 55.3, 106.7, 113.9, 117.8, 120.4, 121.8, 122.5, 124.1,

129.2, 133.4, 136.5, 139.6, 141.9, 156.0, 160.9.

*5.1.5.2. 7-Fluoro-2-(4-methoxyphenyl)-2,5-dihydro-3H-pyrazolo[4,3-c] quinolin-3-one (**4**).* PQ **4** (yellow solid, 164 mg, 90%) was obtained from **13b** (150 mg, 0.59 mmol) according to general procedure D; m.p. decomposition > 300 °C; ^{1}H NMR (400 MHz, DMSO-d_6) δ 3.78 (s, 3H), 7.01 (d, J = 9.2 Hz, 2H), 7.69 (dd, J = 10.1, 2.0 Hz, 1H), 7.88 (d, J = 1.9 Hz, 1H), 8.06 (d, J = 9.2 Hz, 2H), 8.13 (d, J = 8.6 Hz, 1H), 8.74 (s, 1H), 12.80 (br s, 1H); ^{13}C NMR (101 MHz, DMSO-d_6) δ 55.2, 105.8 (d, $^{2}J_{C,F}$ = 25.1 Hz), 106.8, 113.8, 114.7 (d, $J^{2}_{C,F}$ = 27 Hz), 115.5, 120.4, 124.7 (d, $^{3}J_{C,F}$ = 10 Hz), 133.4, 136.7 (d, $J^{1}_{C,F}$ = 11.8 Hz), 139.6, 142.1, 155.9, 160.9, 163.5 (d, $^{1}J_{C,F}$ = 246.9 Hz); HR-MS: m/z 305.0824 [M + H]$^{+}$ (calc. 305.0833, diff. −2.94 ppm).

*5.1.5.3. 7-Chloro-2-(4-methoxyphenyl)-2,5-dihydro-3H-pyrazolo[4,3-c] quinolin-3-one (**5**).* PQ **5** (yellow solid, 110 mg, 92%) was obtained from **13c** (100 mg, 0.37 mmol) according to general procedure D; m.p. decomposition > 330 °C; ^{1}H NMR (400 MHz, DMSO-d_6): δ 3.78 (s, 3H), 7.02 (d, J = 9.2 Hz, 2H), 7.58 (dd, J = 8.6, 2.1 Hz, 1H), 7.73 (d, J = 2.0 Hz, 1H), 8.06 (d, J = 9.2 Hz, 2H), 8.20 (d, J = 8.6 Hz, 1H), 8.77 (s, 1H), 12.78 (s, 1H); ^{13}C NMR (101 MHz, DMSO-d_6) δ 55.3 , 106.8 , 113.9 , 117.5 , 118.8 , 120.4 , 124.0 , 126.5 , 133.4 , 134.1 , 136.4 , 139.8 , 141.9 , 156.0 , 160.9; HR-MS: m/z 326.0708 [M + H]$^{+}$ (calc. 326.0696, diff. −5.64 ppm).

*5.1.5.4. 7-Trifluoromethyl-2-(4-methoxyphenyl)-2,5-dihydro-3H-pyrazolo [4,3-c]quinolin-3-one (**6**).* PQ **7** (yellow solid, 80 mg, 68%) was obtained from **13c** (100 mg, 0.37 mmol) according to general procedure D; m.p. decomposition > 330 °C; ^{1}H NMR (400 MHz, DMSO-d_6) δ 3.79 (s, 3H), 7.02 (d, J = 9.2 Hz, 2H), 7.81 (dd, J = 8.4, 1.6 Hz, 1H), 8.02 (d, J = 1.7 Hz, 1H), 8.09 (d, J = 9.2 Hz, 1H), 8.39 (d, J = 8.4 Hz, 1H), 8.83 (s, 1H). ^{13}C NMR (151 MHz, DMSO-d_6) δ 55.7, 107.3, 114.3, 117.9 (q, $^{3}J_{C,F}$ = 3.9 Hz), 121.0, 122.3, 122.5 (q, $^{3}J_{C,F}$ = 3.2 Hz), 124.0, 124.2 (q, $^{1}J_{C,F}$ = 272.2 Hz), 129.8 (q, $^{2}J_{C,F}$ = 32.5 Hz), 133.9, 136.7, 141.5, 142.2, 156.5, 161.4; HR-MS: m/z 360.0975 [M + H]$^{+}$ (calc. 360.0954, diff. −4.8 ppm).

*5.1.5.5. 7-Methyl-2-(4-methoxyphenyl)-2,5-dihydro-3H-pyrazolo[4,3-c] quinolin-3-one (**7**).* In a vial equipped with a magnetic stirrer and screw cap, PQ **3** (40 mg; 0.1 mmol, 1 equiv.) was suspended in dioxane (1.5 mL). Tetrakis(triphenylphosphine)palladium (0) (0.2 equiv.), K_2CO_3 (2.5 equiv.) and trimethylboroxine (3 equiv.) were added under argon and the reaction mixture was refluxed overnight for 24 h. The reaction mixture was filtered hot trough silica and washed with warm MeOH. The product (yellow solid, 30 mg, 90%) was purified via HPLC; m.p. decomposition > 315 °C; ^{1}H NMR (DMSO-d_6, 400 MHz): δ 2.46 (s, 3H), 3.78 (s, 3H), 7.01 (d, J = 9.2 Hz, 2H), 7.37 (dd, J = 8.3, 1.5 Hz, 1H), 7.49 (s, 1H), 8.09 (dd, J = 8.6, 3.2 Hz, 3H), 8.65 (s, 1H); ^{13}C NMR (DMSO-d_6, 50 MHz): δ 21.8, 55.7, 106.6, 114.2, 116.9, 119.8, 120.7, 122.4, 128.2, 134.1,136.4, 139.7, 140.4, 143.2, 156.2, 161; HR-MS: m/z 306.1254 [M + H]$^{+}$ (calc. 305.1164, diff. −5.24 ppm).

*5.1.5.6. 7-Ethynyl-2-(4-methoxyphenyl)-2,5-dihydro-3H-pyrazolo[4,3-c] quinolin-3-one (**8**).* PQ **14** (150 mg, 0.39 mmol) was dissolved in 15 mL MeOH and K_2CO_3 (107 mg, 0.77 mmol) was added. After stirring for 2.5 h at rt the solvent was removed under reduced pressure. The residue was dissolved in DMSO, filtered through a syringe filter (0.2 µm) and purified by HPLC to give **8** (yellow solid, 104 mg, 0.33 mmol, 85%); m.p. decomposition > 300 °C; ^{1}H NMR (400 MHz, DMSO-d_6): δ 3.78 (s, 3H), 4.47 (s, 1H), 6.97 – 7.06 (m, 2H), 7.58 (dd, J = 8.3, 1.6 Hz, 1H), 7.77 (d, J = 1.5 Hz, 1H), 8.04 – 8.10 (m, 2H), 8.18 (d, J = 8.2 Hz, 1H), 8.76 (s, 1H), 12.82 (br s, 1H); ^{13}C NMR (151 MHz, DMSO-d_6): δ 55.3, 82.6, 83.0, 106.5, 113.9, 119.0, 120.4, 122.6, 122.7, 122.8, 129.1, 133.5, 135.7, 140.1, 142.0, 156.0, 161.0; HR-MS: m/z 316.1090 [M + H]$^{+}$ (calc. 316.1081, diff. −2.88 pm).

*5.1.5.7. 7-Ethyl-2-(4-methoxyphenyl)-2,5-dihydro-3H-pyrazolo[4,3-c] quinolin-3-one (**9**).* PQ **8** (20 mg, 0.063 mmol) was dissolved in 3 mL MeOH and Pd/C (2 mg, 10 wt%) was added. The reaction mixture was stirred at room temperature under hydrogen atmosphere (1 atm). After 3.5 h the solvent was removed under reduced pressure. The residue was dissolved in DMSO, filtered through a syringe filter (0.2 µm) and purified by HPLC to give **9** (yellow solid, 19 mg, 0.60 mmol, 94%); m.p. decomposition > 300 °C; ^{1}H NMR (600 MHz, DMSO-d_6): δ 1.26 (t, J = 7.6 Hz, 3H), 2.77 (q, J = 7.6 Hz, 2H), 3.79 (s, 3H), 6.98 – 7.04 (m, 2H), 7.42 (dd, J = 8.2, 1.6 Hz, 1H), 7.50 – 7.53 (m, 1H), 8.10 (d, J = 9.1 Hz, 2H), 8.13 (d, J = 8.2 Hz, 1H), 8.67 (s, 1H), 12.70 (br s, 1H); ^{13}C NMR (151 MHz, DMSO-d_6): δ 15.3, 28.2, 55.2, 106.1, 113.8, 116.7, 118.2, 120.3, 122.1, 126.6, 133.7, 136.1, 139.4, 142.8, 146.0, 155.8, 161.1; HR-MS: m/z 320.1407 [M + H]$^{+}$ (calc. 320.1394, diff. −4.23 ppm).

*5.1.5.8. 7-Acetyl-2-(4-methoxyphenyl)-2,5-dihydro-3H-pyrazolo[4,3-c] quinolin-3-one (**10**).* PQ **8** (64 mg, 0.2 mmol) was dissolved in 1 mL CF_3CH_2OH. Then H_2O (7.2 µL, 0.4 mmol) and CF_3SO_3H (62 µL, 0.7 mmol) were added and the reaction mixture was heated to 70 °C. After 3 days the solvent was removed under reduced pressure and the residue was dissolved in DMSO, filtered through a syringe filter (0.2 µm) and purified by HPLC to give **10** (yellow solid, 9 mg, 0.027 mmol, 14%). m.p. decomposition > 300 °C; ^{1}H NMR (400 MHz, DMSO-d_6) δ 2.67 (s, 3H), 3.79 (s, 3H), 7.02 (d, J = 9.1 Hz, 2H), 8.05 (dd, J = 8.3, 1.3 Hz, 1H), 8.10 (d, J = 9.1 Hz, 2H), 8.26 – 8.33 (m, 2H), 8.77 (s, 1H), 12.80 (br s, 1H); ^{13}C NMR (151 MHz, DMSO-d_6) δ 26.9, 55.3, 106.4, 113.9, 119.8, 120.5, 122.4, 125.2, 133.5, 137.1, 137.3 141.1, 142.1 (s, C5a/C9b/C1′), 156.0 (s, C4′), 161.0 (s, CO), 197.0; HR-MS: m/z 334.1194 [M + H]$^{+}$ (calc. 334.1186, diff. −2.39 ppm).

*5.1.5.9. 2-(4-Methoxyphenyl)-7-((trimethylsilyl)ethynyl)-2,5-dihydro-3H-pyrazolo[4,3-c]quinolin-3-one (**14**).* PQ **3** (265 mg, 0.72 mmol), Pd$(OAc)_2$ (16 mg, 10 mol%) and PPh_3 (38 mg, 20 mol%) were dissolved in Et_3N (4 mL) and DMF (8 mL). After the reaction apparatus was set under argon, ethynyltrimethylsilane (204 µL, 1.43 mmol) was added and the mixture was heated to 100 °C. After 17 h the reaction mixture was filtered through a syringe (5 mL) filled with cotton and silica (0.5 cm) using MeOH (50 mL) as eluent. The filtrate was concentrated, the residue was redissolved in DMSO and purified by HPLC to give **14** (yellow solid, 160 mg, 0.41 mmol, 58%.; m.p. decomposition > 330 °C; ^{1}H NMR (400 MHz, DMSO-d_6) δ 0.27 (s, 9H), 3.78 (s, 3H), 7.01 (d, J = 9.2 Hz, 2H), 7.55 (dd, J = 8.2, 1.6 Hz, 1H), 7.72 (d, J = 1.6 Hz, 1H), 8.06 – 8.10 (m, 2H), 8.16 (d, J = 8.3 Hz, 1H), 8.75 (s, 1H), 12.70 (br s, 1H); ^{13}C NMR (151 MHz, DMSO-d_6) δ −0.2, 55.3, 96.6, 104.1, 106.4, 113.8, 119.1, 120.4, 122.5, 122.7, 123.0, 129.1, 133.5, 135.9, 140.3, 142.0, 156.0, 161.0; HR-MS: m/z 388.1479 [M + H]$^{+}$ (calc. 388.1476, diff. −0.77 ppm).

5.2. Biological assays

Rat $GABA_A$ receptor concatemeric cDNAs were obtained from Erwin Sigel (University of Bern, Switzerland).

5.2.1. Construction of concatenated receptors

The approach used for subunit concatenation of $GABA_A$ receptors has been described previously[22,29,34,36–40]. We prepared two dual constructs γ2–26–β3, β3–26–α6 and five triple constructs α6–11–β3–26–α6, α6–11–β3–23–α1, α1–10–β3–23–α1, α1–10–β3–26–α6, γ2–26–β3–23–α1. For the design of the linkers, we applied the rule that the sum of the predicted C-terminal protrusion of a preceding subunit and the artificial linker has to be minimally 23 residues in length. Shorter linkers do not result in receptor expression.

5.2.2. Expression of $GABA_A$ receptors in Xenopus oocytes

Capped cRNAs were synthesized (Ambion, Austin, TX, USA) from the linearized plasmids with a cytomegalovirus promotor (pCMV vectors) containing the different subunits, the dual or triple constructs respectively. A poly-A tail of about 400 residues was added to each transcript using yeast poly-A polymerase (United States Biologicals, Cleveland, OH, USA). The concentration of the cRNA was quantified on a formaldehyde gel using Radiant Red stain (Bio-Rad) for visualization of the RNA. Known concentrations of RNA ladder (Invitrogen) were loaded as standard on the same gel. cRNAs were precipitated in ethanol/ isoamylalcohol 19:1, the dried pellet dissolved in water and stored at −80 °C. cRNA mixtures were prepared from these stock solutions and stored at −80 °C. Animal experiments were carried out in strict accordance to the Swiss and Austrian ethical guidelines. Surgery was done under anesthesia, and all efforts were made to diminish animal suffering. *Xenopus laevis* oocytes were prepared, injected and defolliculated as described previously[41,42]. Oocytes were injected with 50 nL of the cRNA solution containing either wild type rat α1/α6β3γ2 subunits at a concentration of 10 :10 :50 nM for the building of loose receptors[43], or the constructed dual and triple concatemers. The dual (β3γ2, β3α6) and triple (α6β3α6, α6β3α1, α1β3α1, α1β3α6, γ2β3α1) constructs were injected each at 50 nM either alone or in different combinations (at a ratio of 25 : 25 nM), resulting in a total of four different concatenated receptors. Injected oocytes were then incubated in modified Barth's solution at 18 °C for at least 24 h before the measurements.

5.2.3. Functional characterization of $GABA_A$ receptors

Currents were measured using a two-electrode voltage clamp amplifier Oocyte clamp OC-725 (Warner Instruments) in combination with a XY-recorder (90% response time 0.1 s) and digitized at 100 Hz using a PowerLab 2/20 (AD Instruments) using the computer programs Chart (ADInstruments GmbH, Spechbach, Germany). Tests with a model oocyte were performed to ensure linearity in the larger current range. The response was linear up to 15 μA. The holding potential was − 80 mV. The perfusion medium contained 90 mM NaCl, 1 mM KCl, 1 mM MgCl2, 1 mM CaCl2, and 5 mM Na-HEPES (pH 7.4). Concentration response curves for GABA were fitted with the equation $I(c) = I_{max}/[1 + (EC_{50}/c)^n]$, where c is the concentration of GABA, EC_{50} the concentration of GABA eliciting half-maximal current amplitude, I_{max} is the maximal current amplitude, I the current amplitude, and n is the Hill coefficient. Maximal current amplitudes (I_{max}) were obtained from the fits of the concentration–response curves. For all receptors studied, modulation by the compounds was measured at a GABA concentration eliciting 1–1.5% of the maximal GABA current amplitude. GABA was applied twice alone for 20–30 s, and then in combination with the different compounds for 20–30 s, until steady state. The duration of washout periods was 4 min in between agonist or agonist/ drug applications to prevent receptor desensitization. At the beginning of the experiments, GABA applications were repeated when the elicited current amplitude altered by > 5%. Potentiation was calculated by the following equation: $(I_{Modulator + GABA}/I_{GABA} - 1) * 100\%$. The perfusion solution (6 mL/min) was applied through a glass capillary with an inner diameter of 1.35 mm, the mouth of which was placed about 0.4 mm from the surface of the oocyte. The perfusion system was cleaned between drug applications by washing with DMSO to avoid contamination. All media contained a final concentration of 0.5% DMSO (v/v) to ensure drug solubility. Concentration dependent potentiation of monotonic sigmoid curves was fitted with the equation $I(c) = I_{max}/[1 + (EC_{50}/c)^n]$, where c is the concentration of the compound, EC_{50} the concentration of the compound eliciting half-maximal current amplitude, I_{max} is the maximal current amplitude, I is the current amplitude, and n the Hill coefficient. Concentration dependent potentiation of biphasic curves was fitted with the equation $I(c) = I_{maxA}/[1 + (EC_{50A}/c)^{nA}] + I_{maxB}/[1 + (EC_{50B}/c)^{nB}]$ where A indicates the more potent phase and B the less potent phase. Hill coefficients were constrained to 1 for better fit in both monophasic and biphasic curves, R^2 was inspected for both models. The biphasic fit was selected for the cases with R^2 closer to 1. All data were analyzed using GraphPad Prism software (version 6.0). All data are from at least two different batches of oocytes. Data represent mean ± SEM.

Acknowledgements

We thank Prof. Dr. Erwin Sigel and his group for hosting Dr. Xenia Simeone and generously leaving her the oocyte setups. Special thanks go to Roland Baur, who generated the concatenated constructs. We gratefully acknowledge the help of Christoph Wiesinger with statistical analysis. This work was supported by the Swiss National Science Foundation Grant 315230_156929/1 and by the Austrian Science Fund Grants I2306 and W1232.

Declaration of Competing Interest

Authors declare no competing interest.

Appendix A. Supplementary data

Supplementary data to this article can be found online at https://doi.org/10.1016/j.bmc.2019.06.006.

References

1. Olsen RW, Sieghart W, International Union of Pharmacology. LXX. Subtypes of gamma-aminobutyric acid(A) receptors: classification on the basis of subunit composition, pharmacology, and function. Update. *Pharmacol Rev.* 2008;60(3):243–260.
2. Sieghart W. Structure and pharmacology of gamma-aminobutyric acidA receptor subtypes. *Pharmacol Rev.* 1995;47(2):181–234.
3. Sieghart W. Allosteric modulation of GABAA receptors via multiple drug-binding sites. *Adv Pharmacol.* 2015;72:53–96.
4. Puthenkalam R, Hieckel M, Simeone X, et al. Structural Studies of GABAA Receptor Binding Sites: Which Experimental Structure Tells us What? *Front Mol Neurosci.* 2016;9:44.
5. Masiulis S, Desai R, Uchanski T, et al. GABAA receptor signalling mechanisms revealed by structural pharmacology. *Nature.* 2019;565(7740):454–459.
6. Ramerstorfer J, Furtmüller R, Sarto-Jackson I, Varagic Z, Sieghart W, Ernst M. The GABA(A) Receptor α+β− Interface: A Novel Target for Subtype Selective Drugs. *J Neurosci Official J Society Neurosci.* 2011;31(3):870–877.
7. Yokoyama N, Ritter B, Neubert AD. 2-Arylpyrazolo[4,3-c]quinolin-3-ones: novel agonist, partial agonist, and antagonist of benzodiazepines. *J Med Chem.* 1982;25(4):337–339.
8. Maldifassi MC, Baur R, Sigel E. Molecular mode of action of CGS 9895 at alpha1 beta2 gamma2 GABAA receptors. *J Neurochem.* 2016;138(5):722–730.
9. Chiou L-CCJ, Ernst M, Fan P-C., et al., Preparation of Ligands Selective to Alpha 6 Subunit-Ccontaining GABAa Receptors and their Methods of Use. WO2016196961 2016.
10. Varagic Z, Ramerstorfer J, Huang S, et al. Subtype selectivity of alpha+beta- site ligands of GABA receptors - identification of the first highly specific positive modulators at alpha6beta2/3gamma2 receptors. *Br J Pharmacol.* 2013.
11. Pirker S, Schwarzer C, Wieselthaler A, Sieghart W, Sperk G. GABA(A) receptors: immunocytochemical distribution of 13 subunits in the adult rat brain. *Neuroscience.* 2000;101(4):815–850.
12. Hortnagl H, Tasan RO, Wieselthaler A, Kirchmair E, Sieghart W, Sperk G. Patterns of mRNA and protein expression for 12 GABAA receptor subunits in the mouse brain. *Neuroscience.* 2013;236:345–372.
13. Nusser Z, Sieghart W, Somogyi P. Segregation of different GABAA receptors to synaptic and extrasynaptic membranes of cerebellar granule cells. *J Neurosci Official J Society Neurosci.* 1998;18(5):1693–1703.
14. Gutiérrez A, Khan ZU, De Blas AL. Immunocytochemical localization of the alpha 6 subunit of the gamma-aminobutyric acidA receptor in the rat nervous system. *J Comp Neurol.* 1996;365(3):504–510.
15. Yang L, Xu T, Zhang K, et al. The essential role of hippocampal alpha6 subunit-containing GABAA receptors in maternal separation stress-induced adolescent depressive behaviors. *Behav Brain Res.* 2016;313:135–143.
16. Puri J, Vinothini P, Reuben J, et al. Reduced GABA(A) receptor α6 expression in the trigeminal ganglion alters inflammatory TMJ hypersensitivity. *Neuroscience.* 2012;213:179–190.
17. Fan PC, Lai TH, Hor CC, et al. The alpha6 subunit-containing GABAA receptor: a novel drug target for inhibition of trigeminal activation. *Neuropharmacology.* 2018;140:1–13.
18. Jechlinger M, Pelz R, Tretter V, Klausberger T, Sieghart W. Subunit Composition and Quantitative Importance of Hetero-oligomeric Receptors: GABA < sub > A < / sub > Receptors Containing α < sub > 6 < /sub > Subunits. *J Neurosci.*

1998;18(7):2449–2457.
19. Vasovic D, Divovic B, Treven M, et al. Trigeminal neuropathic pain development and maintenance in rats are suppressed by a positive modulator of alpha6 GABAA receptors. *Eur J Pain.* 2019;23(5):973–984.
20. Knutson DE, Kodali R, Divović B, et al. Design and Synthesis of Novel Deuterated Ligands Functionally Selective for the γ-Aminobutyric Acid Type A Receptor (GABAAR) α6 Subtype with Improved Metabolic Stability and Enhanced Bioavailability. *J Med Chem.* 2018;61(6):2422–2446.
21. Treven M, Siebert DCB, Holzinger R, et al. Towards functional selectivity for α6β3γ2 GABAA receptors: a series of novel pyrazoloquinolinones. *Br J Pharmacol.* 2018;175(3):419–428.
22. Minier F, Sigel E. Techniques: Use of concatenated subunits for the study of ligand-gated ion channels. *Trends Pharmacol Sci.* 2004;25(9):499–503.
23. Andersson JD, Halldin C. PET radioligands targeting the brain GABAA /benzodiazepine receptor complex. *J Labelled Comp Radiopharm.* 2013;56(3–4):196–206.
24. Varagic Z, Wimmer L, Schnurch M, et al. Identification of novel positive allosteric modulators and null modulators at the GABA receptor alpha + beta- interface. *Br J Pharmacol.* 2013.
25. Yokoyama N, Ritter B, Neubert AD. 2-Arylpyrazolo[4,3-c]quinolin-3-ones: a novel agonist, a partial agonist and an antagonist of benzodiazepines. *J Med Chem.* 1982;25(4):337–339.
26. Liu W, Wang H, Li CJ. Metal-Free Markovnikov-Type Alkyne Hydration under Mild Conditions. *Org Lett.* 2016;18(9):2184–2187.
27. Chiou LC, Lee HJ, Ernst M, et al. Cerebellar alpha6 -subunit-containing GABAA receptors: a novel therapeutic target for disrupted prepulse inhibition in neuropsychiatric disorders. *Br J Pharmacol.* 2018;175(12):2414–2427.
28. Baumann SW, Baur R, Sigel E. Subunit arrangement of GABAA receptors. *J Biol Chem.* 2001;276(39):36275–36280.
29. Baumann SW, Baur R, Sigel E. Forced subunit assembly in α1β2γ2 GABAA receptors. Insight into the absolute arrangement. *J Biol Chem.* 2002;277(48):46020–46025.
30. Zhu S, Noviello CM, Teng J, et al. Structure of a human synaptic GABAA receptor. *Nature.* 2018;559(7712):67–72.
31. Maric D, Maric I, Wen X, et al. GABAA receptor subunit composition and functional properties of Cl- channels with differential sensitivity to zolpidem in embryonic rat hippocampal cells. *J Neurosci Official J Society Neurosci.* 1999;19(12):4921–4937.
32. Simeone X, Siebert DCB, Bampali K, et al. Molecular tools for GABAA receptors: High affinity ligands for beta1-containing subtypes. *Sci Rep.* 2017;7(1):5674.
33. Gutierrez A, Khan ZU, De Blas AL. Immunocytochemical localization of the alpha 6 subunit of the gamma-aminobutyric acidA receptor in the rat nervous system. *J Comp Neurol.* 1996;365(3):504–510.
34. Minier F, Sigel E. Positioning of the α-subunit isoforms confers a functional signature to gamma-aminobutyric acid type A receptors. *PNAS.* 2004;101(20):7769–7774.
35. Zhang P, Zhang W, Liu R, Harris B, Skolnick P, Cook JM. Synthesis of novel imidazobenzodiazepines as probes of the pharmacophore for “diazepam-insensitive” GABAA receptors. *J Med Chem.* 1995;38(10):1679–1688.
36. Baumann SW, Baur R, Sigel E. Subunit arrangement of gamma-aminobutyric acid type A receptors. *J Biol Chem.* 2001;276(39):36275–36280.
37. Baumann SW, Baur R, Sigel E. Individual properties of the two functional agonist sites in GABA(A) receptors. *J Neurosci Official J Society Neurosci.* 2003;23(35):11158–11166.
38. Baur R, Kaur KH, Sigel E. Structure of alpha6 beta3 delta GABA(A) receptors and their lack of ethanol sensitivity. *J Neurochem.* 2009;111(5):1172–1181.
39. Baur R, Kaur KH, Sigel E. Diversity of structure and function of α1α6β3δ GABAA receptors: comparison with α1β3δ and α6β3δ receptors. *J Biol Chem.* 2010;285(23):17398–17405.
40. Kaur KH, Baur R, Sigel E. Unanticipated structural and functional properties of delta-subunit-containing GABAA receptors. *J Biol Chem.* 2009;284(12):7889–7896.
41. Sigel E. Properties of single sodium channels translated by Xenopus oocytes after injection with messenger ribonucleic acid. *J Physiol.* 1987;386:73–90.
42. Sigel E, Minier F. The Xenopus oocyte: system for the study of functional expression and modulation of proteins. *Mol Nutr Food Res.* 2005;49(3):228–234.
43. Boileau AJ, Baur R, Sharkey LM, Sigel E, Czajkowski C. The relative amount of cRNA coding for gamma2 subunits affects stimulation by benzodiazepines in GABA(A) receptors expressed in Xenopus oocytes. *Neuropharmacology.* 2002;43(4):695–700.